Accepted Manuscript

Influence of network structure on the degradation of poly(ether)amine-cured epoxy resins by inorganic acid

Jonathon D. Tanks, Masatoshi Kubouchi, Yoshihiko Arao

PII: S0141-3910(18)30323-9

DOI: 10.1016/j.polymdegradstab.2018.10.011

Reference: PDST 8660

To appear in: *Polymer Degradation and Stability*

Received Date: 10 July 2018

Revised Date: 13 September 2018

Accepted Date: 10 October 2018

Please cite this article as: Tanks JD, Kubouchi M, Arao Y, Influence of network structure on the degradation of poly(ether)amine-cured epoxy resins by inorganic acid, *Polymer Degradation and Stability* (2018), doi: https://doi.org/10.1016/j.polymdegradstab.2018.10.011.

Influence of network structure on the degradation of poly(ether)amine-cured epoxy resins by inorganic acid

Jonathon D. Tanks*, Masatoshi Kubouchi, Yoshihiko Arao

School of Materials and Chemical Technology, Tokyo Institute of Technology

* Corresponding author, Tel.: (863)703-6540; E-mail address: tanks.j.aa@m.titech.ac.jp

Abstract

In this paper, we investigate the case of bisphenol-type epoxy crosslinked with poly(ether)amine, immersed in sulfuric acid at elevated temperature. The results show that very high equilibrium mass-change (up to 40%) is observed, and that amine protonation is largely responsible for this behavior. When the acid solution concentration is 5mass% or higher, alcohol dehydration and aromatic ether cleavage reactions occur by excess acid (after amine protonation). A mechanistic degradation model is proposed, which requires no empirical parameters and accounts for polymer network structure differences. The model is supported by calculating the theoretical crosslink density using gravimetric data of penetrated acid at equilibrium.

1. Introduction

In addition to being one of the most common matrix resins for fiber- and particle-reinforced composites, epoxy is also used as a lining material for metallic

and concrete structure in a variety of industries, including automotive, marine, chemical, and civil [1,2]. Thus, while epoxy used in aircraft fuselage applications may not encounter harsh chemical environments such as aqueous acid, epoxy linings and epoxy-based composites used in chemical storage tanks or pipelines must withstand sustained exposure to such conditions for many years. Examples include hydrochloric, acetic, citric, phosphoric, and sulfuric acids, at temperatures ranging from ambient to 100 °C [1].

Polymer resins containing ester functional groups often undergo hydrolysis reactions, which can be accelerated by acid or base catalysts [3-8]. As this includes epoxy cured by anhydride, amine curing agents are a widely used alternative because they are much more stable against water and also allow for curing at lower temperature compared to anhydride [1,2]. However, despite their water stability, amines are known to react with sulfuric acid to form a quaternary ammonium salt at the crosslink sites, which can have detrimental effects on the epoxy resin depending on the composition and curing conditions [2,9-11]. Consequently, experimental data pertaining to diffusion kinetics of sulfuric acid in amine-cured epoxy resin is also lacking in the literature, but the available studies have shown that it tends to be proportional to the square-root of time, similar to Fickian diffusion [9,10]. The salt formation mechanism discussed in

the available literature likely does not follow Fick's law, but the proportionality to $\sqrt{t}$ makes it convenient for applying a standard analytical model to estimate diffusion parameters.

Dang et al. [12,13] discussed the degradation of bisphenol-diglycidyl-ether (DGEBF)/1,8-*p*-menthanediamine reacted with nitric acid for chemical recycling applications. Nitric acid (HNO_3), which is a strong acid and oxidizing agent, attacks the C–N bonds at the crosslinks and nitrates the benzene rings [12]. Similarly, Ma et al. [14] proposed a chemical recycling method at atmospheric pressure for amine-cured epoxy, wherein a combination of glacial acetic acid and hydrogen peroxide caused C–N bond cleavage at crosslinks as well as ether cleavage. In nearly all examples from the literature, C–N bond cleavage by acid requires oxidation in addition to protonation. For amine-cured epoxy exposed to sulfuric acid, no significant chemical change was reported but a decrease in mechanical properties was observed, leading the authors to speculate that C–N bond cleavage may follow quaternary ammonium salt formation [1,2,4,5,9,10,15]. Additionally, although extremely high mass-uptake of sulfuric acid in amine-cured epoxy—between 30-40% (by mass), compared to 2-5% for water—has been observed numerous times [2,9,10], the only suggestion in the literature is that the difference in molecular weight between water and sulfuric

acid is responsible for this increase. However, no clear experimental evidence nor theoretical scheme has been proposed to address either of these observations.

In this paper, we discuss the degradation mechanism of bisphenol-F epoxy cured with poly(ether)amine exposed to aqueous sulfuric acid, as a model system. Different network structures are achieved by using different lengths of polyether chains, while the general crosslinking scheme is kept approximately constant. We show that the equilibrium acid absorption is determined by the polymer/acid reactions, which is confirmed by FTIR and crosslink density calculations. The three-way reaction scheme proposed here is not found anywhere in the literature, and we consider this to be the missing piece in a long-unfinished puzzle. These results provide insight into how amine-cured epoxy degrades by inorganic acid and how network structure affects this process, as well as how the equilibrium acid absorption (i.e., maximum uptake) can be predicted based on measurable structural parameters such as crosslink density. While the anticipated application of our work is epoxy degradation analysis, it is possible that some of the proposed mechanisms here also apply to epoxy recycling efforts.

2. Materials and methods

2.1. Materials

The main epoxy resin used was a commercial bisphenol F-diglycidyl ether

(DGEBF, Epiclon 830), coupled with an aliphatic-type poly(oxypropylene)diamine hardener (Jeffamine D230). The chemical structures of these monomers, along with bisphenol A epoxy (DGEBA) and poly(oxypropylene)triamine hardener, are shown in Figure 1. The environmental solution consisted of reagent-grade H_2SO_4 (98%) and deionized water.

A second set of specimens included bisphenol-A (DGEBA) epoxy, as well as polyether-amines with different polyether chain lengths ($2.5 \leq n \leq 50$); in addition to diamine, long-chain triamine were also mixed with short-chain diamine.

2.2. Specimen preparation

The same procedure was followed for all specimens, with amine mixtures according to Table 1. The naming convention used for each series is determined by the epoxy type (BPA or BPF) and the amine type (di- or triamine).The primary specimens in this study, FD1, were prepared by adding D230 hardener to DGEBF at a mass ratio of 100:33.8 and mixed at room temperature for 15 min at 600 rpm. After degasing the mixture for approximately 15 min, it was poured into pre-heated steel molds and cured at a schedule of 80 °C for 12 hr, followed by 120 °C for 12 hr. After cooling to room temperature, the cured epoxy plates were removed from the molds and cut with a water-cooled carbide blade into

rectangular specimens, having dimensions of 60×20×2 mm (*l*×*w*×*h*). All specimens were lightly polished and washed with soap and water to remove mold release and other debris that could interfere with the surface adsorption phenomenon necessary for liquid penetration.

2.3. Immersion conditions

Aqueous solutions of H_2SO_4 were prepared by mixing with deionized water at concentrations from 0.1–20 mass%. The solutions were kept in a water bath at temperatures of 40, 60, and 80 °C, with the exception of 20mass% being held at only 80 °C. All specimens were dried in a desiccator for one week prior to immersion.

2.4. Experimental techniques

The amount of penetrated acid solution was approximated by gravimetric analysis. The change in mass of the specimens over time was measured on a digital balance (precision ±0.1 mg) and calculated according to $M(t) = (M_w - M_0)/M_0$, where M_0 is the initial mass before immersion and M_w is the current mass at time *t*. These measurements were taken very carefully and consistently to reduce errors: the specimens were removed from the solution and towel-dried, then the measurements were made after the mass stabilized (i.e., once the surface was just at the point of saturation but without excess moisture), and

finally the specimens were immediately returned to the solutions. After reaching the maximum uptake level, referred to as the equilibrium or saturation uptake, the specimens were dried completely under vacuum at 40 °C until the mass stabilized (typically at least 100 hr), and all measurements were repeated for the dry state. At least three specimens were tested for each condition, and the results were averaged to ensure accurate representation.

Fourier-transform infrared (FTIR) spectra of FD1 specimens were taken using FTIR-ATR (Shimadzu AIM-8000R) at a resolution of 4 cm^{-1} and a minimum of 60 scans averaged per spectrum. The spectra from at least three locations on a specimen were averaged to ensure consistent trends in the data.

In order to assess the effects of the penetrated acid on the mechanical properties, three-point bending tests were performed using FD1 specimens on an electromechanical universal testing machine (Shimadzu Autograph AGS), using a fixed span length of 40 mm and a loading rate of 1 mm/min.

For all specimens, the crosslink density ν_{exp} was calculated according to Eq. (1), using the rubber elasticity theory [16] with thermomechanical analyzer (TMA) measurements:

$$\nu_{exp} = \frac{E'}{3RT'} \tag{1}$$

where E' is the rubbery modulus at T', R is the gas constant, and $T' = T_g +$

40 °C. Experimentally determined values for ν_{exp} and T_g are given in Table 1.

3. Experimental results

3.1 Equilibrium mass uptake

Representative results of gravimetric analysis are shown in Figure 2(a). Whereas water shows the typical equilibrium uptake of 3% (by mass), H_2SO_4 solution reaches well over ten times that value. Furthermore, no mass-loss was observed for any condition even after 4000 hr. Acid concentrations of 5, 10, and 20mass% at 60 °C were selected for demonstrating the slight increase in equilibrium acid uptake with increasing concentration for all resin series, as seen in Figure 2(b); it should be noted that no significant difference in the equilibrium uptake exists for 60 °C and 80 °C. While amine-cured epoxy immersed in pure water typically reaches equilibrium uptake values less than 5% (relative to epoxy initial mass), H_2SO_4 solutions exhibit very high mass-change ranging between 27-40% (wet condition). The equilibrium uptake in the dry condition indicates the approximate mass of penetrated acid, neglecting penetrated water. In order to understand the relationship between equilibrium uptake and the polymer network structure, we show the same data plotted against measured crosslink density in Figure 2(c) for all epoxy series in both wet and dry states. Clearly, although a slight upward trend is visible, the data is scattered and no clear

relationship is evident. This is the starting point to our analysis described in Section 4.

3.2 FTIR spectroscopy

The aromatic C=C peak at 1508 cm^{-1} was chosen as the standard for normalizing each spectra in Figure 3, since these peak should remain relatively unchanged during acid immersion. Crosslinks are signified by C–N stretch between 1070-1180 cm^{-1} (aliphatic 3° amine). The sulfate ion appears in the peak around 1135 cm^{-1}, which affects nearby peaks and makes it difficult to identify bands of interest. The small peak located around 1725 cm^{-1} signifies carbonyl. Several less obvious changes can be seen with some effort: the aryl ether peak around 1240 cm^{-1} is crowded by the phenolic C–O peak nearby at 1210 cm^{-1} [17], the peak for secondary alcohol C–O around 1090 cm^{-1} seems to decrease and hide in the large aliphatic ether peak at 1110 cm^{-1} [18], and the primary alcohol C–O peak at 1020 cm^{-1} drastically increases. These interpretations form the basis for the reaction schemes we propose in Section 4.

3.3 Mechanical properties

While other polymer systems may show mass-loss in addition to strength-loss, such as polyester immersed in KOH [4,5], amine-cured epoxy shows no mass-loss to be used as an indicator of degradation. However, acid

penetration does lead to reduced mechanical properties, as shown in Figure 4. The flexural modulus in the wet and dry conditions are shown for various temperatures and acid concentrations. The wet condition data primarily show the plasticization effect of a high volume of penetrated water in the polymer network, which increases chain mobility through polar interactions. Conversely, the dry condition data shows the actual behavior of the material, with minimal plasticization effects. The observed trend is a steady decrease until roughly 20% mass-change, and finally a more sharp reduction for the highest mass-change region. This indicates that chemical reactions occur over time in the material.

4. Degradation model

4.1 Reaction scheme

For the tertiary amine crosslink, we consider only protonation without C–N bond cleavage. Rather, the most likely reactions to occur are shown in Figure 5. Strong acids such as H_2SO_4 can cleave ethers (aliphatic in **1**, aryl in **2**) with high enough concentration and temperature, yielding an amino-propanediol (**1**, **2**) and phenol (**2**). The aliphatic ether is more readily attacked than the aryl ether due to resonance, but neither reaction is guaranteed to occur. A more likely pathway is shown in **3**, where first the acid easily dehydrates the secondary alcohol to form an enol ether intermediate, which is readily hydrolyzed under

acidic conditions into phenol and aldehyde. This cannot be proven without further chemical analysis (such as solid-NMR), but in theory this pathway is more likely to occur under the conditions of our study, and the formation of a small amount of aldehyde corroborates the FTIR spectra for the peak around 1725 cm^{-1}. We propose that chain scission by inorganic acid does indeed occur, but not through the commonly assumed C–N bond [4,12]. Furthermore, the amount of chain scission is small enough that mass loss is not observed due to the relatively large dangling chains that remained attached at crosslink sites, unlike mass loss typical of anhydride-cured epoxy undergoing hydrolysis [4-7].

4.2 Theoretical calculation of crosslink density

If the penetrated acid reacts with the polymer network as described in Section 4.1, then we should be able to calculate the theoretical crosslink density from the mass change results (Fig. 2). This is because amine protonation is the primary driver of inorganic acid diffusion in the polymer, so by default there is one amine for every crosslink point; the other reactive functional groups are divided into crosslink sites.

We define the crosslink sites using a simplified 2D schematic in Figure 6. Since the poly(ether)amine chains are the same length or longer than the DGEBF/DGEBA chains, we make a distinction between the actual *crosslink point*

(i.e., tertiary amine connecting two epoxy chains to the polyether chain) and the *crosslink site*, which is the region surrounding the crosslink point such that each chain is divided symmetrically in terms of functional groups. For example, in Figure 7, the two marked regions **(1)** and **(2)** both contain an equal number of functional groups from the connecting chains: one tertiary amine, two secondary alcohols, and $n/2 + 2$ ethers (2 aromatic, $n/2$ aliphatic), where n is the repeat unit for the di- and tri-amine chains. The length of the green poly(ether)amine chain depends on n for each formulation in Table 1.

The crosslink density can be calculated theoretically by

$$\nu_{calc} = \frac{M_{\infty,d}\rho_0}{m_{w,A}}\frac{a_H}{\overline{f}} \tag{2}$$

where $M_{\infty,d}$ is the equilibrium mass-change after drying, ρ_0 is the initial polymer density, $m_{w,A}$ is the molecular weight of the acid, a_H is the number of dissociated protons per acid molecule, and $\overline{f}$ is the functionality (i.e., average number of reactive polymer functional groups at each crosslink site). This equation essentially converts mass of penetrated acid into moles of acid per unit volume, which is then converted into moles of crosslinks. This equation is generalized so that the influence of network structure is included, and so that polyprotic acids may be treated equally. However, determination of $\overline{f}$ requires the full understanding of all reaction schemes that may occur, as this essentially

represents the proton consumption per crosslink.

Initially, we assumed $a_H = 2$ for H_2SO_4 due to its diprotic nature, but the correct definition should consider the dissociation constant for each series in the case of polyprotic acids. For strong acids, we can assume $K_{a1} \approx 1$ (actually $\gg 1$), while K_{a2} and K_{a3} can be found in various chemistry reference tables. Thus we write

$$a_H = \sum_{i=1}^{k} K_{ai} \tag{3}$$

for any inorganic acid having k protons per acid molecule. Using appropriate values for H_2SO_4 yields $a_H = 1.01$, which represents the statistical average number of protons dissociated per acid molecule—it does not have to be an integer. This effectively halves the calculated crosslink density from our original assumption of $a_H = 2$. We also initially assumed that only the amine protonation reaction occurs, resulting in a one-to-one molar consumption of acid protons ($\overline{f} = 1$). The resulting comparison between calculated and experimental crosslink density is shown in Figure 7. Clearly, there is a linear trend for two distinct groups: series with only D230 ($n = 2.5$) or D400 ($n = 6.3$) correlate to higher ν_{calc} values, while series including T3000 ($n = 50$) and D2000 ($n = 33$) form a linear trend with lower ν_{calc} values. However, in both cases the theoretical result significantly overestimates the experimental values. Thus, we

next considered only two reactions: amine protonation and alcohol elimination. Figure 8 shows the new result using the correct value of a_H and changing the functionality to include two alcohols at each crosslink site, so that $\overline{f} = 3$. Although much closer in agreement with experiments, two problems remain. First, the functionality is too high; i.e., the assumed proton consumption per crosslink site is overestimated. Second, the short- and long-chain amine series are still separated, yet showing linear trends. We infer from this that $\overline{f}$ must be between 1 and 3, and it may be a non-integer. Additionally, if only alcohol elimination occurs, the enol ether product is unlikely to be stable in acidic conditions and there would be no chain scission, leaving the degradation mechanism unclear.

Finally, we developed an expression for $\overline{f}$ based on the concept of competing priority for proton consumption, using the reaction schemes described in Section 4.1. We must first determine whether $\overline{f}$ must be the same for all epoxy series or it varies. Based on the first two trials using fixed integer values for all series, it follows that $\overline{f}$ must vary depending on the network structure. In that case, the part of the structure that changes most significantly for each series must be identified. Due to the design of experiments in this study, only the number of aliphatic ethers in the crosslinker constitutes a significant variation; we neglect

any influence of the epoxy type or whether the crosslinker is a di- or triamine.

Consider that the proposed reaction schemes do not necessarily need to occur at every crosslink site—with the exception of amine protonation, which will continue until all available sites have reacted. Furthermore, we propose that pathway **3** is the most plausible, so that two reactions must occur in sequence—dehydration and hydrolysis. The relative amount of reactive alcohol per crosslink site, with respect to both aromatic and aliphatic ether, is given by

$$f_{\mathrm{OH}} = \frac{n_{\mathrm{OH}}}{n_{\mathrm{ROR}} + n_{\mathrm{ROR'}}} \tag{4}$$

where n_{OH} is the number of alcohols, n_{ROR} is the number of aromatic ethers, and $n_{\mathrm{ROR'}}$ is the number of aliphatic ethers. Likewise, the relative amount of reactive aromatic ether with respect to alcohol and aliphatic ether is expressed by

$$f_{\mathrm{ROR}} = \frac{n_{\mathrm{ROR}}}{n_{\mathrm{OH}} + n_{\mathrm{ROR'}}}. \tag{5}$$

Finally, because the amine protonation takes priority in the proton consumption hierarchy, we define the reactivity of the amine crosslink point at each crosslink site as

$$f_{\mathrm{N^+}} = 1. \tag{6}$$

In this study, all of the prepared epoxy resins contain bisphenol-type difunctional epoxies, so $n_{\mathrm{OH}} = n_{\mathrm{ROR}} = 2$, while $n_{\mathrm{ROR'}}$ varies according to the appropriate

mixture of the individual n values for each crosslinker (Table 1). Combining Eqs. (4)-(6), the average functionality of each crosslink site accounting for the network structure takes the form

$$\overline{f} = f_{\mathrm{N^+}} + f_{\mathrm{OH}} + f_{\mathrm{ROR}} \tag{7}$$

which can be simplified to the arithmetic relation

$$\overline{f} = 1 + \frac{4}{2 + n_{\mathrm{ROR'}}}. \tag{8}$$

Eq. (8) accounts for the network structure wherein the length of poly(ether)amine chains is the controlling factor, and it can be solved simply using the values of n provided by the chemical manufacturer; see Table 2 for values of $n_{\mathrm{ROR'}}$ and $\overline{f}$. Thus, the final result of our theoretical estimation of crosslink density is given in Figure 9. The issue mentioned previously regarding the gap between long- and short-chain poly(ether)amines has been resolved, which is clear from the single linear trend observed for all epoxy series.

We also found that the length of the PEA chain has a strong influence on the portion of water absorbed by epoxy. Consider that the ratio of equilibrium uptake values for the dry and wet conditions ($M_{\infty,d}/M_{\infty,w}$) can represent a qualitative estimate of the hydrophilicity of the network. This relative hydrophilicity is plotted against $n_{\mathrm{ROR'}}$ in Figure 10. A more hydrophilic network will hold more water (relative to the amount of absorbed acid) compared to a less hydrophilic

network. This may also imply that the local concentration of aqueous acid at any given point in the network is higher for the case of shorter PEA chains, which would also contribute to the apparent higher reactivity for those networks.

We assume the primary source of error to be the dry mass-change measurement, since some water might be effectively trapped due to high concentration of sulfate ions. Thus, the actual equilibrium uptake in the dry state would be slightly lower than our results show. However, this has no influence on the basis of our analysis—i.e., acid degradation mechanism and the effect of network structure; it only affects the accuracy of quantitative results in comparison with experimental values.

5. Conclusions

In this study, we proposed a degradation mechanism of bisphenol-type epoxy crosslinked with poly(ether)amines exposed to non-oxidizing inorganic acid. These reaction schemes and the corresponding analysis of crosslink density are, to our knowledge, not reported in any of the previous literature. By studying eight different series of epoxy resins, with various crosslinker chain length and either DGEBA or DGEBF, it was possible to determine the influence of polyether chain length on the equilibrium acid uptake. Protonation of the amine crosslinks is the primary driver for acid uptake, which will progress until all available sites

are reacted when the concentration of the acid solution is sufficiently high (in this study, 5mass% showed very little difference from 20mass%). We propose that aryl ether is cleaved by acid indirectly, involving both alcohol dehydration and hydrolysis of the resulting intermediate. The validity of the degradation model is yet unknown due to lack of in-depth chemical analysis, but we consider that the corroboration of crosslink density calculations, FTIR analysis, and gravimetric analysis support our proposed mechanism to some degree. This approach can be used to study diffusion behavior, strength reduction, and service life prediction for epoxy resins exposed to acidic environments.

Acknowledgments

JT gratefully acknowledges the financial support of the Ministry of Education, Sports, Science, Culture and Technology (MEXT) of Japan.

References

1. Møller VB, Dam-Johansen K, Frankær SM, Kiil S. Acid-resistant organic coatings for the chemical industry: A review. J Coat Technol Res 2017;14(2):279-306.
2. Sembokuya H, Negishi Y, Kubouchi M, Tsuda K. Corrosion behavior of epoxy resin cured with different amount of hardener in corrosive solutions. Mater Sci Res Int 2003;9:230-234.

3. F Xiao GZ, Shanahan MER. Water absorption and desorption in an epoxy resin with degradation. J Polym Sci Pol Phys 1997;35(16):2659-2670.
4. Tsuda K. Behavior and mechanisms of degradation of thermosetting plastics in liquid environments. J Jpn Petrol Inst 2007;50(5):240-248.
5. Hojo H, Tsuda K, Kubouchi M, Kim D-S. Corrosion of plastics and composites in chemical environments. Metal Mater 1998;4(6):1191-1197.
6. Capiel G, Uicich J, Fasce D, Montemartini PE. Diffusion and hydrolysis effects during water aging on an epoxy-anhydride system. Polym Degrad Stab 2018;152:165-171.
7. Capiel G, Miccio LA, Montemartini PE, Schwarts GA. Water diffusion and hydrolysis effect on the structure and dynamics of epoxy-anhydride networks. Polym Degrad Stab 2017;143:57-63.
8. Marella VV, Throckmorton JA, Palmese GR. Hydrolytic degradation of highly crosslinked polyaromatic cyanate ester resins. Polym Degrad Stab 2014;104:103-111.
9. Abacha N, Kubouchi M, Sakai T, Tsuda K. Diffusion behavior of water and sulfuric acid in epoxy/organoclay nanocomposite. J Appl Polym Sci 2009;112(2):1021-1029.
10. Abacha N, Kubouchi M, Tsuda K, Sakai T. Performance of

epoxy-nanocomposite under corrosive environment. Express Polym Lett 2007;1(6):364-369.

11. Abastari, Sakai T, Sembokuya H, Kubouchi M, Tsuda K. Study on Permeation Behavior and Chemical Degradation of PA66 in Acid Solution. Polym Degrad Stab, 2007;92:379-388.
12. Dang W, Kubouchi M, Yamamoto S, Sembokuya H, Tsuda K. An approach to chemical recycling of epoxy resin cured with amine using nitric acid. Polymer 2002;43(10):2953-2958.
13. Dang W, Kubouchi M, Sembokuya H, Tsuda K. Chemical recycling of glass fiber reinforced epoxy resin cured with amine using nitric acid. Polymer 2005;46(6):1905-1912.
14. Ma Y, Kim D, Nutt SR. Chemical treatment for dissolution of amine-cured epoxies at atmospheric pressure. Polym Degrad Stab 2017;146:240-249.
15. Nazemi MK, Valix M. Evaluation of acid diffusion behavior of amine-cured epoxy coatings by accelerated permeation testing method and prediction of their service life. Prog Organ Coat 2016;97:307-312.
16. Khonakdar HA, Morshedian J, Wagenknecht U, Jafari SH. An investigation of chemical crosslinking effect on properties of high-density polyethylene. Polymer 2003;44(15):4301-4309.

17. Yao F-L, Sheng S-R, Jiang J-W, Liu X-L, Song C-S. Soluble copoly(aryl ether ether ketone ketone)s containing xanthene and hexafluoroisopropylidene moieties. J Fluor Chem 2012;144:176-181.

18. Deng Y, Li S, Zhao J, Zhang Z, Zhang J, Yang W. Crystallizable and tough aliphatic thermoplastic poly(ether urethane)s synthesized through a non-isocyanate route. RCS Advan 2014;4:43406-43414.

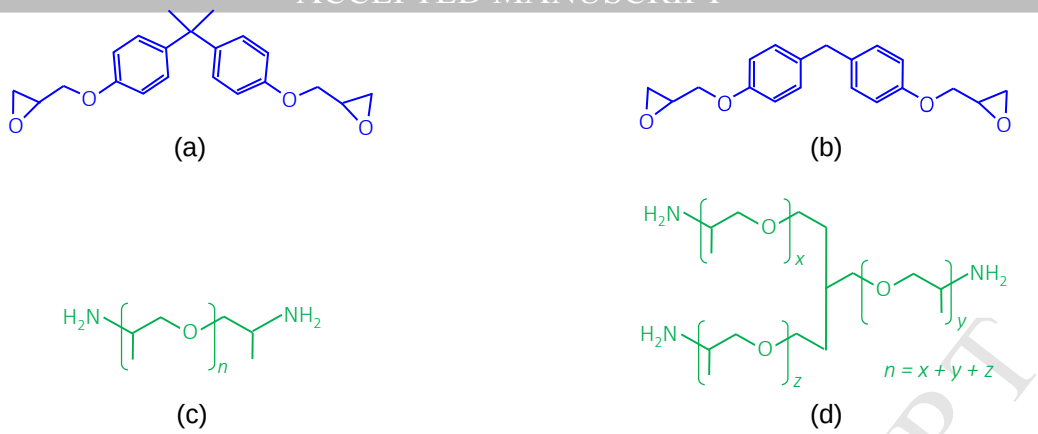

Figure 1. (a) DGEBA, (b) DGEBF, (c) poly(oxypropylene)diamine, (d) poly(oxypropylene)triamine.

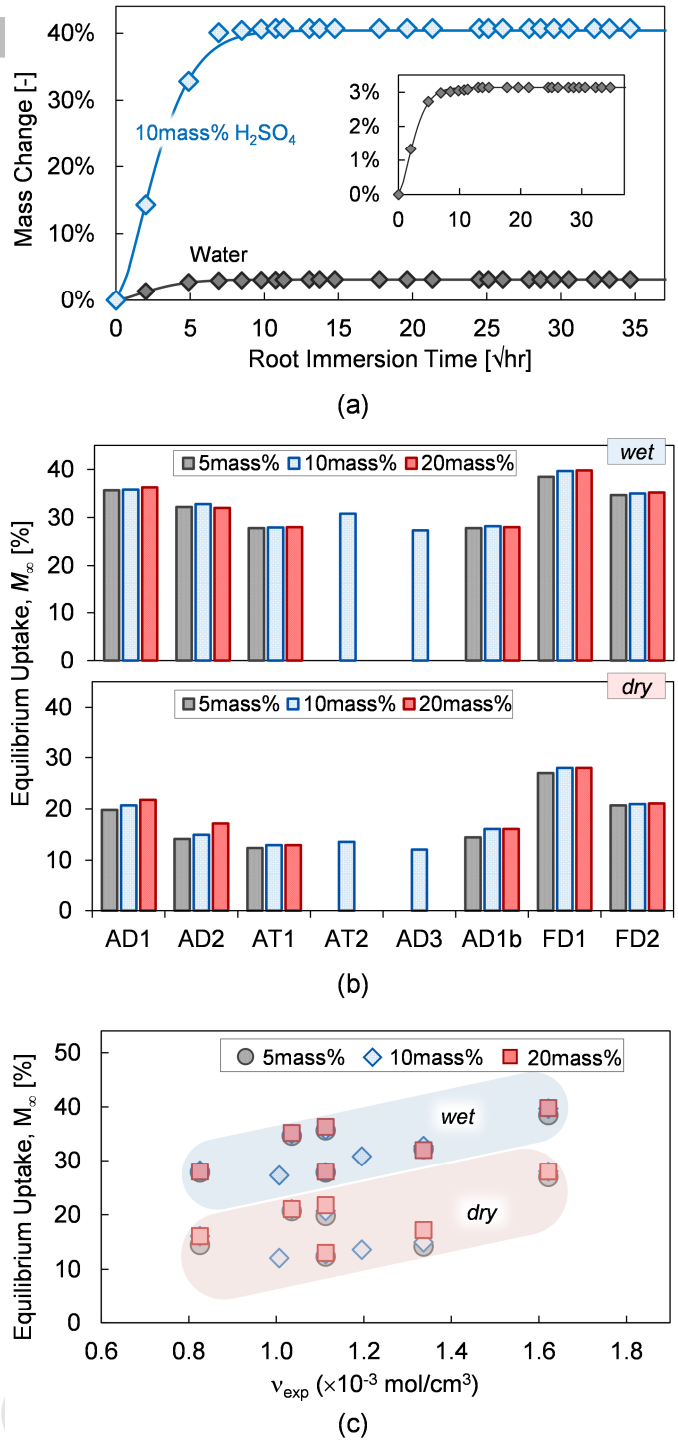

Figure 2. Mass uptake of H_2SO_4 at 80 °C: (a) representative gravimetric curve for FD1 (magnified curve for water shown in inset), (b) equilibrium uptake for all epoxy series in wet and dry states, and (c) relationship between equilibrium uptake and crosslink density for wet and dry states.

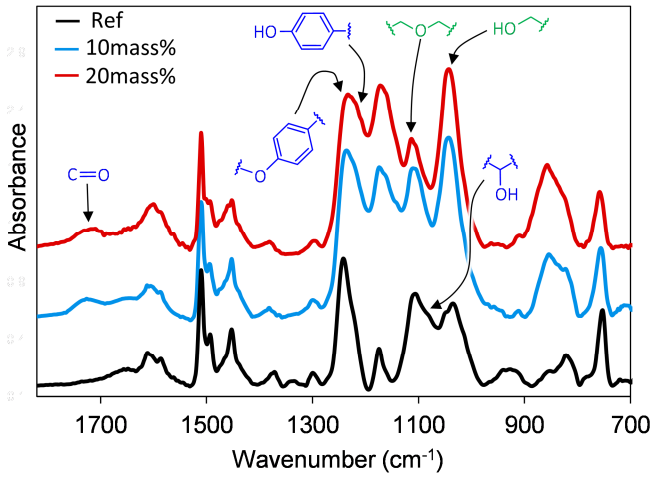

Figure 3. FTIR spectra for FD1 after reaching saturation in various concentrations of H_2SO_4 at 80 °C.

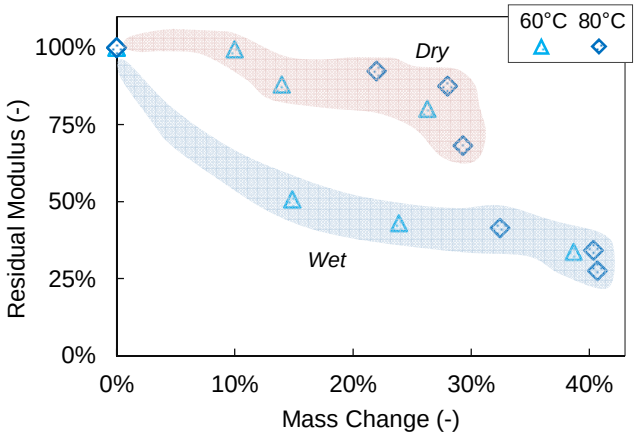

Figure 4. Residual flexural modulus for FD1 in 10mass% H_2SO_4 at different points of pre-equilibrium mass change.

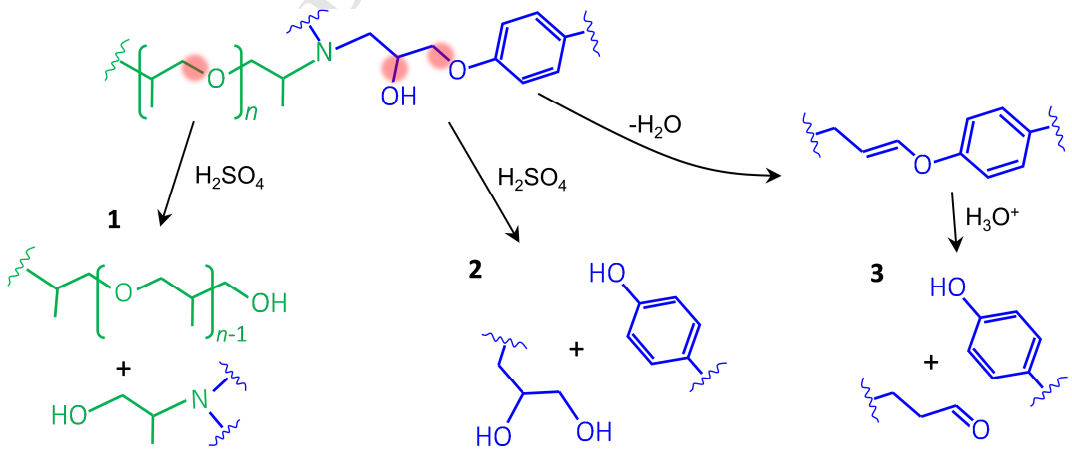

Figure 5. Reaction scheme for degradation of poly(ether)amine-cured epoxy: **1** aliphatic ether cleavage to form 3-amino-1,2-propanediol; **2** aryl ether cleavage to form phenol and 3-amino-1,2-propanediol; **3** alcohol dehydration to form enol ether, which is hydrolyzed into phenol and aldehyde.

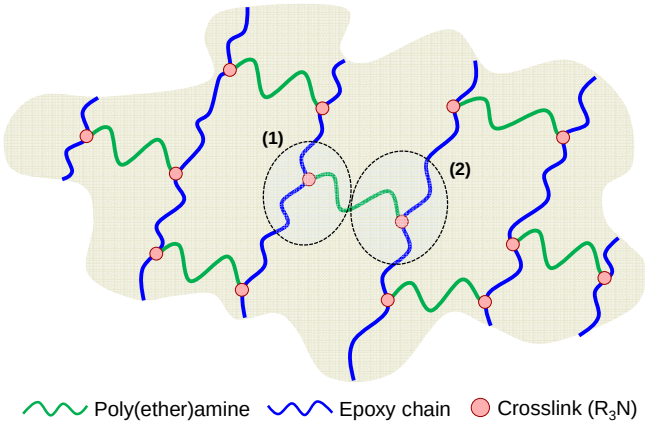

Figure 6. Simplified 2D network showing the definition of *crosslink site* for the calculation of theoretical crosslink density based on the reaction scheme in Section 4.1.

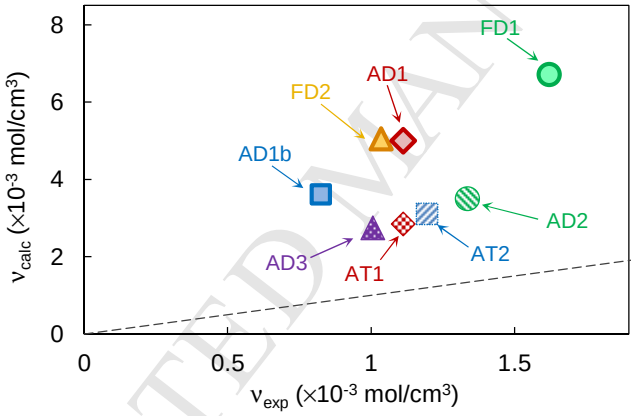

Figure 7. Calculated crosslink densities with $a_H = 2$ and $\overline{f} = 1$. *(dashed line is 1:1)*

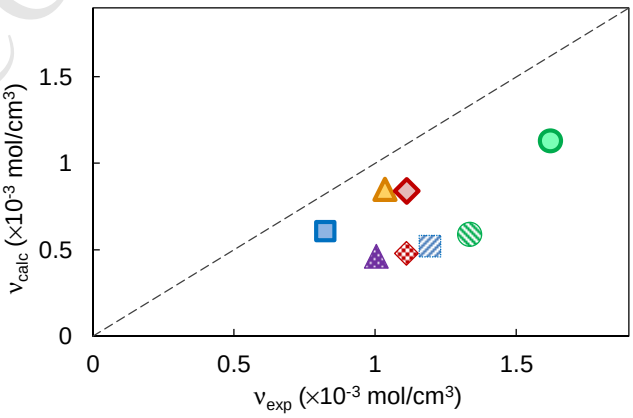

Figure 8. Calculated crosslink densities with $a_H = 1.01$ and $\overline{f} = 3$. *(dashed line is 1:1)*

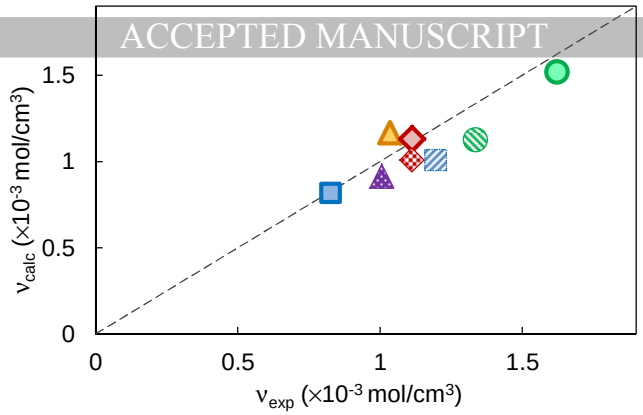

Figure 9. Calculated crosslink densities with $a_H = 1.01$ and $\overline{f}$ according to Table 2. *(dashed line is 1:1)*

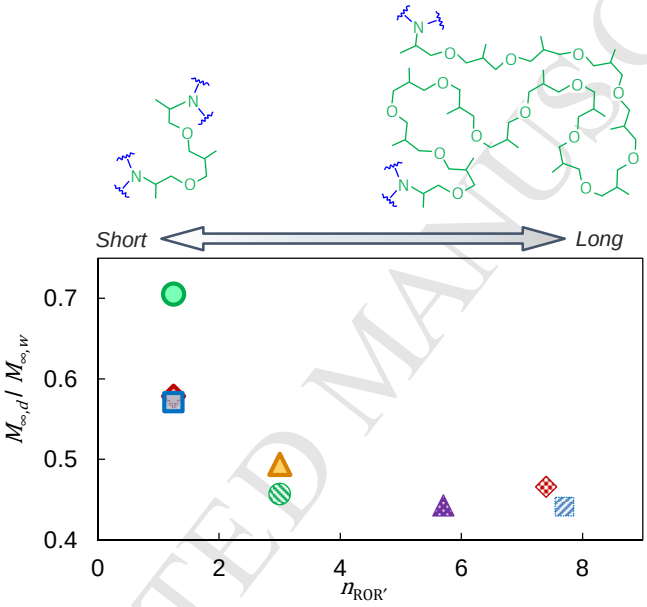

Figure 10. Relationship between relative hydrophilicity and ether repeat unit $n_{\mathrm{ROR}'}$.

Table 1 Composition of epoxy/polyamine networks.

Series ID	Epoxy resin [a]	Crosslinker (mol%)	ν_{exp} (×10^{-3}mol/cm^3)	T_g (°C)
FD1	DGEBF	D230(100%)	1.621	90.3
FD2	DGEBF	D400(100%)	1.035	47.2
AD1	DGEBA	D230(100%)	1.112	102.2
AD2	DGEBA	D400(100%)	1.336	60.3
AD3	DGEBA	D400(80%)+D2000(20%)	1.006	33.2
AT1	DGEBA	D400(80%)+T3000(20%)	1.112	36.2
AT2	DGEBA	D400(90%)+T3000(10%)	1.195	46.8
AD1b	DGEBA'	D230(100%)	0.825	104.3

[a] *DGEBA = Epomik R140, DGEBA' = Epikote 834; DGEBF = Epomik R110 or Epiclon 830*

Table 2 Network structure parameters for calculating the functionality of each epoxy series.

Mixture series	n_{OH}	n_{ROR}	$n_{ROR'}$	$\overline{f}$
FD1	2.00	2.00	1.25	2.23
FD2	2.00	2.00	3.00	1.78
AD1	2.00	2.00	1.25	2.23
AD2	2.00	2.00	3.00	1.78
AD3	2.00	2.00	5.70	1.51
AT1	2.00	2.00	7.40	1.42
AT2	2.00	2.00	7.70	1.55
AD1b	2.00	2.00	1.25	2.23

- Equilibrium acid uptake in amine-cured epoxy is determined by reactions in the epoxy chain.

- Amine protonation, alcohol elimination, and ether cleavage consume acid protons in order of priority.

- Crosslink density calculations demonstrate the relationship between acid uptake and degradation reactions.